ACTA UNIVERSITATIS AGRICULTURAE ET SILVICULTURAE MENDELIANAE BRUNENSIS

Volume LIX 26 Number 1, 2011

EXPERIMENTAL DETERMINATION OF TEMPERATURES OF THE INNER WALL OF A BOILER COMBUSTION CHAMBER FOR THE PURPOSE OF VERIFICATION OF A CFD MODEL

P. Trávníček, R. Kukla, T. Vítěz, Jan Mareček

Received: October 18, 2010

Abstract

TRÁVNÍČEK, P., KUKLA, R, VÍTĚZ, T., MAREČEK, J.: *Experimental determination of temperatures of the inner wall of a boiler combustion chamber for the purpose of verification of a CFD model.* Acta univ. agric. et silvic. Mendel. Brun., 2011, LIX, No. 1, pp. 235–242

The paper focuses on the non-destructive method of determination of temperatures in the boiler combustion chamber. This method proves to be significant mainly as regards CFD (Computational Fluid Dynamics) simulations of combustion processes, in case of which it is subsequently advisable to verify the data calculated using CFD software application with the actually measured data. Verification of the method was based on usage of reference combustion equipment (130 kW) which performs combustion of a mixture of waste sawdust and shavings originating in the course of production of wooden furniture. Measuring of temperatures inside the combustion chamber is – considering mainly the high temperature values – highly demanding and requires a special type of temperature sensors. Furthermore, as regards standard operation, it is not possible to install such sensors without performing structural alterations of the boiler. Therefore, for the purpose of determination of these temperatures a special experimental device was constructed while exploiting a thermal imaging system used for monitoring of the surface temperature of outer wall of the reference boiler. Temperatures on the wall of the boiler combustion chamber were determined on the basis of data measured using the experimental device as well as data from the thermal imaging system. These values might serve for verification of the respective CFD model of combustion equipment.

temperature on the inner wall of a combustion chamber, combustion equipment, thermal imaging measurement, CFD model of the combustion process, heat transmission coefficient

Verification of measured data by the means of their comparison with data calculated using CFD software and their validation is essential in connection with creation of CFD models in various types of software applications. Numerous methods (Grace *et al.*, 2004; Stamou *et al.*, 2006) may be used for this purpose – depending on the type of matter to be resolved (Miltner *et al.*, 2007; Lorente *et al.*, 1996). The method presented in this paper may be exploited primarily in case of combustion equipment in case of which it is difficult to determine the actual temperature inside the combustion chamber, mainly due to its rather high values. Depending on the type of combustion equipment and combustion conditions, the respective temperature might reach up to 750°C (Lavric *et al.*, 2004; Novozhilov *et al.*, 1996). However, the temperature of the outer surface of the boiler reaches max. 100 °C and it is easily measurable. Should the outer surface temperature be known, it is also essential to know the heat transmission coefficient. It is a material constant which is, however, dependent on the temperature, i.e. it varies in connection with the temperature (Tomba *et al.*, 2000). The heat transmission coefficient values form the content of material data sheets (value range: 20 °C–1000 °C). Nevertheless, two unknown factors

remain in the calculation – the heat flow rate and the surface temperature of lining inside the combustion chamber. Due to this fact it was essential to construct an experimental device using which it would be possible to determine relation between the boiler outer surface temperature and the temperature of the inner wall of a combustion chamber.

Measuring of the surface temperature of the boiler outer surface was based on the method of contactless measurement using a thermal imaging system, which uses energy of infrared radiation for temperature measurement purposes. Infrared radiation is subdivided into three ranges (short-wave, medium and remote infrared range) within the wave length range between 0.78 μm and 1000 μm (Sakai *et al.*, 1994). Increasing temperature of the source results in increasing of the energy of infrared radiation and the radiation maximums shift towards shorter wave lengths; for example, the maximum radiation of a human body is 9,3 μm (Vaško, 1963). The applied thermographic system conducts measurements within the range of 7.5 to 13 μm (wave length) and –20 °C to 500 °C (reference temperature range). Following measurement of the outer surface temperature and determination of temperature differences in the external device, each measured point is subsequently allocated to an algorithm used for calculation of the thermal field of the inner wall of the combustion chamber. The aforementioned thermal field may serve for verification of CFD results based on simulation of combustion processes.

MATERIAL AND METHODS

Determination of Material Emissivity

A measuring point, at which the temperature was measured using a OMEGA HH11 contact thermometer (accuracy of temperature measurement: ± 0.1 °C), was created on the casing of the combustion equipment. The most significant prerequisite was to prevent fluctuation of temperature in the course of time. The aforementioned point was also monitored using FLIR E320 thermal camera. In case that the temperature values proved to differ, the temperature in the thermal camera was calibrated by the means of setting up the emissivity value in the user interface of this device. The final emissivity value was determined at the time when the temperature values on both the devices were balanced.

Thermal Imaging Measurement

In addition to emissivity of the monitored material, it is also essential (for thermal imaging measurement purposes) to measure the air temperature, air humidity and distance from the monitored object. The air temperature and humidity were measured using OMEGA RH81 thermo-hygrometre featuring the temperature measurement accuracy of ± 1°C and humidity measurement accuracy of ± 4% (at the temperature of 25 °C and relative humidity within the range of 10–90%). The temperature and humidity were measured in the close vicinity of the thermal camera and combustion equipment, and the arithmetic mean was subsequently calculated on the basis of these values.

The thermal screening measurement was conducted at a constant distance from the combustion equipment. Three photographs were created in the course of one hour. The distance of the camera from the combustion equipment was determined using Leica DISTO^{tm} A5 laser EDM device (measurement accuracy: ± 1.5 mm at a distance between 0.2 and 200 m). The thermal imaging measurement as such was conducted using FLIR ThermaCAM E320 thermal camera (FOV: 25°).

The average temperature of the surface was calculated using ThermaCAM QuickReport software in which each pixel of the video recording was allocated to one temperature value. An arithmetic mean was subsequently created on the basis of all values.

Experimental Measurement

The basis for the experimental device was a layer of lining material (fire clay) and insulation layers consisting of Peril, a porous material. Both these materials are used in the reference source. This layer of material was subsequently insulated using mineral wool and placed on a resistance heater (1200 W). Temperatures of the inner and outer surfaces of the layer were read at the time interval of 1 second by two T-type thermoelectric couples (measurement range: –200 °C to 400 °C) which were connected to ADAM, an external data collection module. The typical deviation was ± 1 °C while the maximum deviation was ± 1.5 °C. Measured data were subsequently evaluated using ControlWeb software. For a picture of the experimental device see Fig. 1.

Calculation

A network of 188 elementary areas was created on the photograph from thermal screening. As regards each of the elementary areas, ThermaCAM QuickReport software was used to determine the respective average temperature. The surface temperature of the inner section of the combustion chamber pertaining to each respective elementary area was subsequently calculated using the following formula derived from the experimental measurement:

$$t_1 = \frac{\ln\left(\frac{t_2}{22.256}\right)}{0{,}0019} \; [^{\circ}\mathrm{C}], \qquad (1)$$

where:

t_1.... surface temperature of inner part of combustion chamber

t_2.... surface temperature of outer part of boiler.

This formula is valid for boiler surface temperatures in the range between 23 °C and ∞. In case of calculation of a temperature lower than 23 °C, the following formula is to be used:

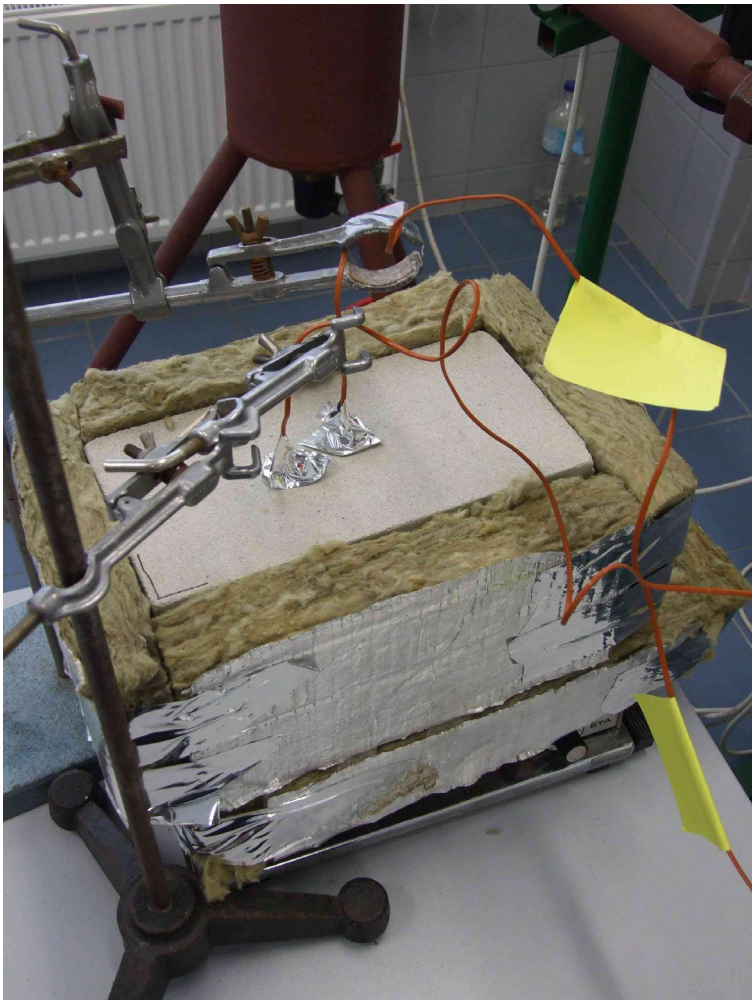

1: *Experimental device*

$$t_1 = 504.92\ln(t_2) - 1553.8\ [^{\circ}C], \quad (2)$$

where:
t_1.... surface temperature of inner part of combustion chamber,S
t_2.... surface temperature of outer part of boiler.

RESULTS AND DISCUSSION

Thermal Imaging Measurement

For an overview of measured limit conditions that are essential for correct evaluation of the thermal imaging measurement see Tab I.

I: *Measured limit conditions essential for correct evaluation of the thermal imaging measurement*

Type of Limit Condition	Value	Unit
Emissivity	0.89	–
Reflected temperature	34.8	°C
Air temperature	29.7	°C
Air humidity	17.6	%
Distance	3	m

Based on the thermal imaging measurement it was determined that the average temperature of the monitored area was 60.9 °C. The maximum temperature in the area was 90.9 °C and the minimum temperature in the area was 16.4 °C. The minimum temperature in the area was lower than the air temperature due to the fact that a small part of the boiler surface was cooled by the floor. However, this anomaly did not affect any additional calculations. For the temperature distribution field see Fig. 2.

Experimental Measurement

The heat transmission coefficient dependence on the temperature was converted into a chart on the basis of the data sheets pertaining to individual materials used for lining of the boiler. For the heat transmission coefficient dependence on the temperature in case of fire clay see Fig. 3; for the heat transmission coefficient dependence on the temperature in case of the insulation material (Peril) see Fig. 4. Both the figures documents the fact that the function characterizing the respective dependence is exponential; the determination coefficient applicable to the function characterizing the heat transmission coefficient

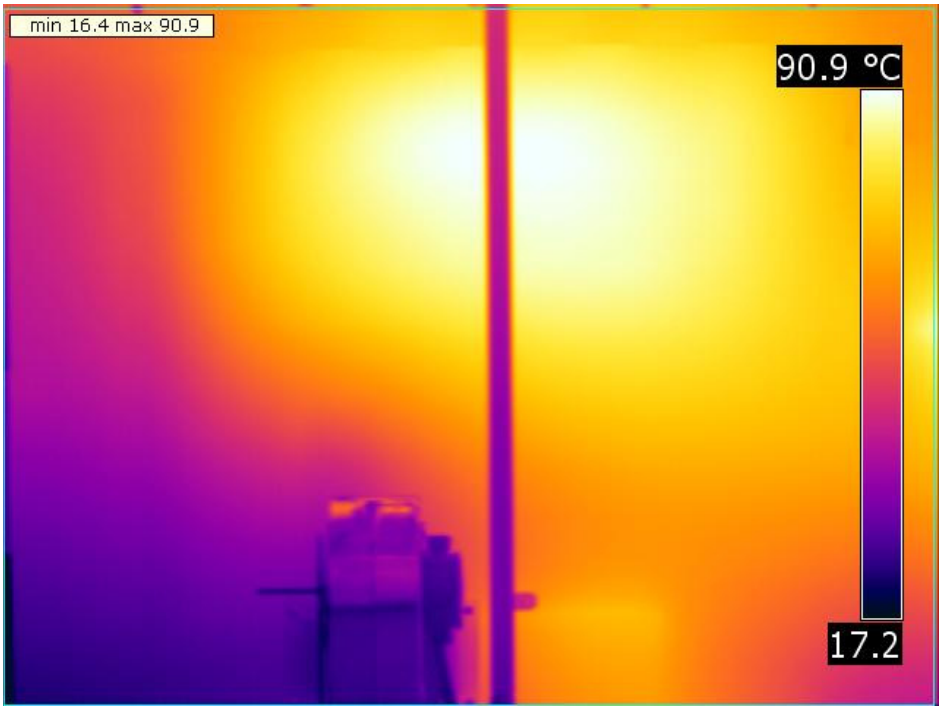

2: *Temperature distribution field at front side of the combustion equipment*

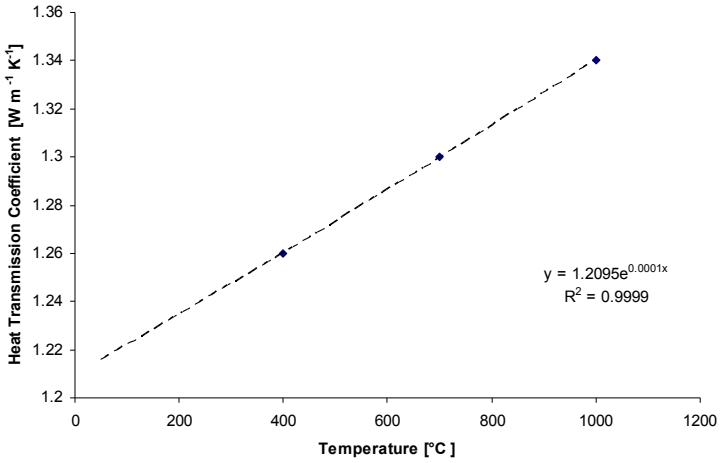

3: *Heat transmission coefficient dependence on the temperature – fire clay*

dependence on the temperature in case of fire clay is $R^2 = 0.99$ while in case of Peril it is $R^2 = 0.97$.

The experimental device performed measurements in the temperature range of 25 °C to 400 °C. In total, more than 33,000 values were recorded and evaluated. For the dependence between the inner surface temperature of a material layer and outer surface temperature of a material layer see Fig. 5. The following stage of measurement was supposed to comprise heating of a layer of material using a gas burner in order to determine the temperature dependence in the range of 400–700 °C. However, due to safety reasons the experiment was terminated (the propane-butane cylinder was overheated). However, the chart in Fig. 5 documents the fact that the inner and outer surfaces calculated using the formula of $y = 22.256e^{0.0019x}$ are in compliance with the data presented about temperature values inside a combustion chamber in specialized journals (Lavric *et al.*, 2004; Novozhilov *et al.*, 1996). Therefore, the highest temperature measured using the thermal camera (90.9 °C) is to be allocated to the value of 740.7 °C.

Calculation

For an auxiliary network of cells containing average temperatures from the respective area see Fig. 3. For temperatures allocated to individual numbers of elementary areas see Tab. II. This table also shows

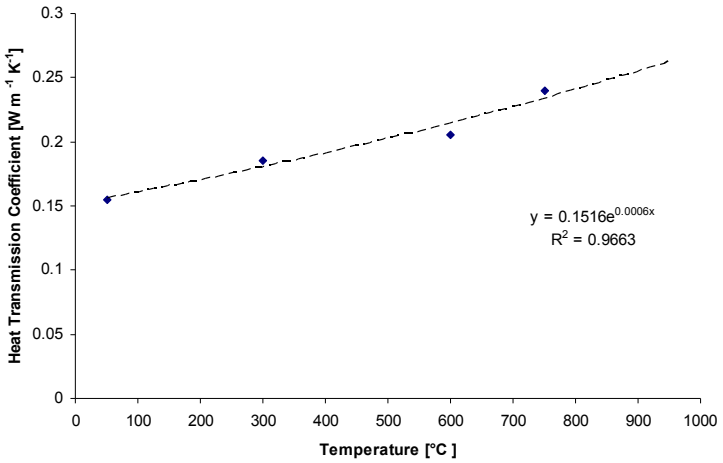

4: *Heat transmission coefficient dependence on the temperature – Peril*

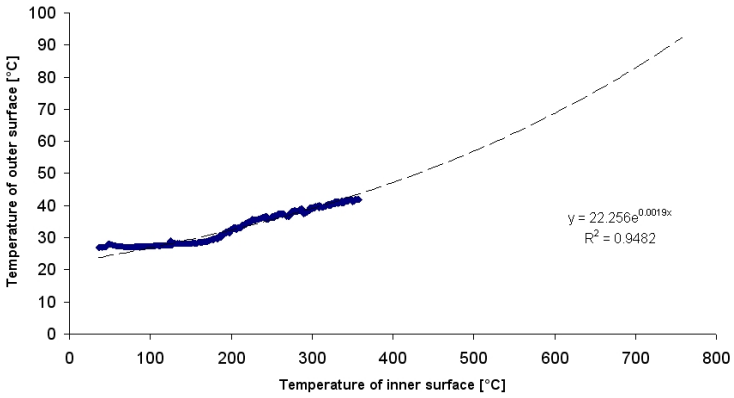

5: *Measured values: temperatures of inner and outer surfaces of the layer of material*

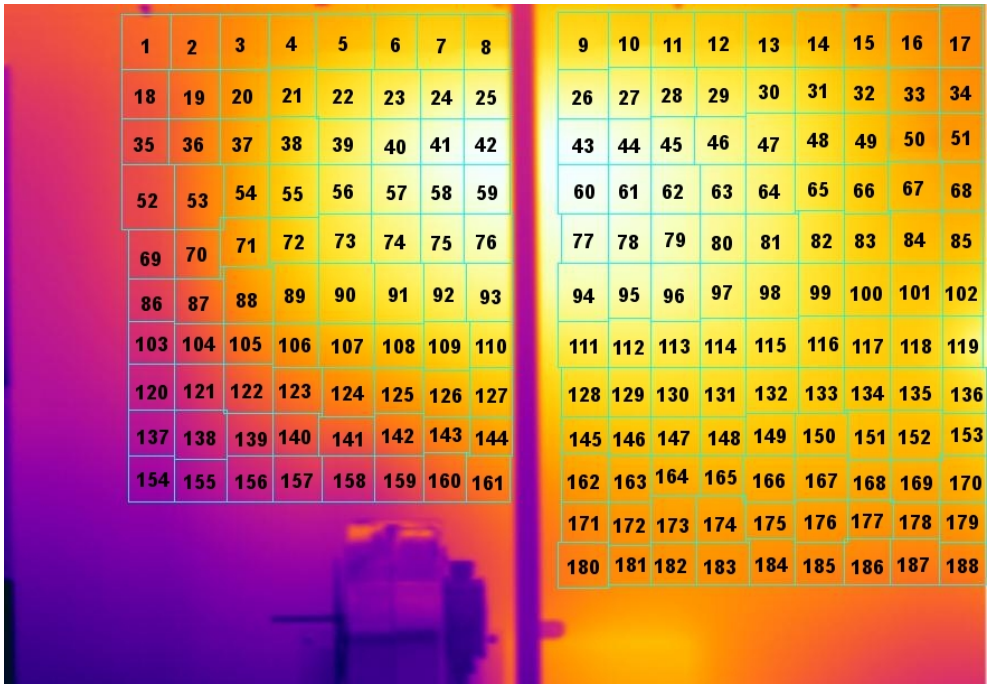

6: *Auxiliary network containing numbers of elementary areas*

II: *Average temperatures in individual cells*

Number	Temp.[°C]	Number	Temp.[°C]	Number	Temp.[°C]	Number	Temp.[°C]	Number	Temp.[°C]
1	56.9	39	85.3	77	89.2	115	79.8	153	73.7
2	60.3	40	86.6	78	88.8	116	77.5	154	37.7
3	68.0	41	89.0	79	87.7	117	75.5	155	40.5
4	72.4	42	89.8	80	86.0	118	75.5	156	44.3
5	75.6	43	90.1	81	83.5	119	80.5	157	46.9
6	77.3	44	89.2	82	79.6	120	44.3	158	47.7
7	77.6	45	87.7	83	75.6	121	48.9	159	51.4
8	78.7	46	85.8	84	72.4	122	55.2	160	56.7
9	77.9	47	83.5	85	71.8	123	59.9	161	60.6
10	77.2	48	79.2	86	51.7	124	63.3	162	67.2
11	76.4	49	74.3	87	55.9	125	66.9	163	68.7
12	74.7	50	68.7	88	64.9	126	69.8	164	70.1
13	72.1	51	66.0	89	71.9	127	72.5	165	70.4
14	69.2	52	53.0	90	77.2	128	77.0	166	69.9
15	66.2	53	59.9	91	80.9	129	77.9	167	69.6
16	64.0	54	68.5	92	83.6	130	78.1	168	68.9
17	66.8	55	76.4	93	84.4	131	77.6	169	68.6
18	54.9	56	82.7	94	87.0	132	76.7	170	70.1
19	59.8	57	86.6	95	87.1	133	75.3	171	63.3
20	66.5	58	88.8	96	86.3	134	74.1	172	65.2
21	73.1	59	89.7	97	84.7	135	74.2	173	66.6
22	83.0	60	90.3	98	82.2	136	77.4	174	67.0
23	85.3	61	89.6	99	79.0	137	41.1	175	66.6
24	86.2	62	88.3	100	75.9	138	44.8	176	66.2
25	86.5	63	86.4	101	74.4	139	49.8	177	65.7
26	85.8	64	84.1	102	76.0	140	53.5	178	65.3
27	84.1	65	79.8	103	47.2	141	55.6	179	66.1
28	82.4	66	75.1	104	52.6	142	59.1	180	61.7
29	80.8	67	70.8	105	60.3	143	63.2	181	64.0
30	77.0	68	68.7	106	66.0	144	66.3	182	64.9
31	72.5	69	53.0	107	70.6	145	72.0	183	64.8
32	67.5	70	58.3	108	74.3	146	73.2	184	64.0
33	64.9	71	67.6	109	77.2	147	73.9	185	63.0
34	67.9	72	75.4	110	79.0	148	73.9	186	62.1
35	53.7	73	81.0	111	82.5	149	73.5	187	61.3
36	59.5	74	84.6	112	83.1	150	72.7	188	61.7
37	69.9	75	86.8	113	82.6	151	71.9		
38	76.0	76	87.2	114	81.7	152	71.8		

that the maximum temperature of the network surface is 90.3 °C.

For values calculated using the formula (1) and allocated to individual elementary areas see Tab. III. The maximum temperatures reach approximately 730 °C, which is in compliance with the specialized journals that specify – in connection with burning of biomass – similar temperature values applicable to the inner section of the combustion chamber (Lavric *et al.*, 2004; Novozhilov *et al.*, 1996).

III: *Calculated temperatures of the inner wall of the combustion chamber*

Number	Temp.[°C]	Number	Temp.[°C]	Number	Temp.[°C]	Number	Temp.[°C]	Number	Temp.[°C]
1	494.2	39	707.3	77	730.8	115	672.2	153	630.3
2	524.7	40	715.2	78	728.4	116	656.8	154	277.5
3	588.0	41	729.6	79	721.9	117	643.0	155	315.2
4	621.0	42	734.3	80	711.6	118	643.0	156	362.4
5	643.7	43	736.1	81	696.1	119	676.8	157	392.5
6	655.4	44	730.8	82	670.9	120	362.4	158	401.4
7	657.5	45	721.9	83	643.7	121	414.4	159	440.7
8	664.9	46	710.4	84	621.0	122	478.2	160	492.3
9	659.5	47	696.1	85	616.6	123	521.2	161	527.3
10	654.8	48	668.2	86	443.7	124	550.3	162	581.8
11	649.3	49	634.6	87	484.9	125	579.4	163	593.4
12	637.4	50	593.4	88	563.4	126	601.7	164	604.0
13	618.8	51	572.3	89	617.3	127	621.7	165	606.2
14	597.2	52	456.8	90	654.8	128	653.4	166	602.5
15	573.9	53	521.2	91	679.4	129	659.5	167	600.2
16	556.1	54	591.8	92	696.7	130	660.9	168	594.9
17	578.6	55	649.3	93	701.7	131	657.5	169	592.6
18	475.4	56	691.0	94	717.7	132	651.3	170	604.0
19	520.3	57	715.2	95	718.3	133	641.7	171	550.3
20	576.2	58	728.4	96	713.4	134	633.2	172	565.9
21	626.0	59	733.8	97	703.6	135	633.9	173	577.0
22	692.9	60	737.3	98	687.8	136	656.1	174	580.2
23	707.3	61	733.2	99	666.9	137	323.0	175	577.0
24	712.8	62	725.5	100	645.8	138	368.4	176	573.9
25	714.6	63	714.0	101	635.3	139	424.0	177	569.9
26	710.4	64	699.8	102	646.5	140	461.8	178	566.7
27	699.8	65	672.2	103	395.8	141	482.0	179	573.1
28	689.1	66	640.3	104	452.8	142	514.2	180	536.8
29	678.8	67	609.2	105	524.7	143	549.5	181	556.1
30	653.4	68	593.4	106	572.3	144	574.7	182	563.4
31	621.7	69	456.8	107	607.7	145	618.1	183	562.6
32	584.1	70	507.0	108	634.6	146	626.8	184	556.1
33	563.4	71	584.9	109	654.8	147	631.8	185	547.8
34	587.2	72	642.4	110	666.9	148	631.8	186	540.2
35	463.7	73	680.1	111	689.7	149	628.9	187	533.4
36	517.7	74	702.9	112	693.5	150	623.2	188	536.8
37	602.5	75	716.5	113	690.4	151	617.3		
38	646.5	76	718.9	114	684.6	152	616.6		

SUMMARY

The paper focuses on the possibility of exploitation of alternative methods of verification of data from a CFD model of the combustion process. It was based on use of a thermal imaging system and calculation of the temperature of the inner wall of a combustion chamber on the basis of experimental measurements. The reference combustion equipment (130 kW) used for burning of a mixture of sawdust and shavings was used for this purpose. The lining of this source comprises a layer of fire clay and a layer of porous insulation material known under the trade name of Peril. The Values determining the heat transmission coefficient dependence on the respective temperatures were presented in material data sheets obtained from manufacturers. As regards both the materials, this dependence

proved to be exponential. Considering this fact, deliberations were based on the presumption that the function determining the dependence of temperature of the inner wall of the heated surface on the temperature of the outer surface would also be exponential. Validity of this presumption was confirmed by experimental measurements using experimental equipment, which was constructed for this purpose. Due to safety reasons, measurements were conducted solely within the temperature range of 23–400 °C. The measured values served as a basis for specification of the determination coefficient function ($R^2 = 0.95$) that was subsequently used for calculation of surface temperatures inside the combustion chamber within the range of 400–1 000 °C. Based on the calculations, the maximum temperature was 737 °C. This value proves to be in compliance with the specialized journals (Lavric *et al*., 2004; Novozhilov *et al*., 1996). In order to perform a verification of data calculated using CFD simulation, it was necessary to create a network of points for which the average temperature was determined on the thermal photograph. This network may contain any number of elementary areas to which temperatures will be allocated – always on the basis of the accuracy which is essential to be reached in the course of calculations. A network of 188 elementary areas was created within the scope of the paper. In case of data verification, a network with featuring the identical scope would be created within the graphical representation of calculations of the numerical simulation. Subsequently, individual temperatures would be compared.

REFERENCES

GRACE, J., R., TAGHIPOUR, F., 2004: Verification and validation of CFD models and dynamic similarity for fluidized beds. Powder Technology, 139: 99–110.

LAVRIC, E., D., KONNOV, A., A., DE RUYCK, J., 2004: Dioxin levels in wood combustion–a review. Biomass and Bioenergy, 26: 115–145.

LORENTE, S., PETIT, M., JAVELAS, R., 1996: Simplified analytical model for thermal transfer in vertical hollow brick. Energy and Buildings, 24: 95–103.

MILTNER, M., MILTNER, A., HARASEK M., FRIEDL, A., 2007: Process simulation and CFD calculations for the development of an innovative baled biomass-fired combustion chamber. Applied Thermal Engineering, 27: 1138–1143.

NOVOZHILOV, V., MOGHTADERI, B., FLETCHER, D., F., KENT, J. H., 1996: Computational Fluid Dynamics Modelling of Wood Combustion. Fire Safety Journal, 27: 69–84.

SAKAI, N., HANZAWA, T., 1994: Applications and advances in far-infrared heating in Japan. Trends in Food Science & Technology, 51: 357–362.

STAMOU, A., KATSIRIS, I., 2006: Verification of a CFD model for indoor airflow and heat transfer. Building and Environment, 41: 1171–1181.

TOMBA, A., G., CAVALIERI, A., L., 2000: Evaluation of the heat transfer coefficient in thermal shock of alumina disks. Materials Science and Engineering, A276: 76–82.

VAŠKO, A., 1963: Infračervené záření a jeho užití. SNTL, 25–271.

Address

Ing. Petr Trávníček, Dr. Ing. Radovan Kukla, Ing. Tomáš Vítěz, Ph.D., prof. Ing. Jan Mareček, DrSc., Ústav zemědělské, potravinářské a environmentální techniky, Mendelova univerzita v Brně, Zemědělská 1, 613 00 Brno, Česká republika, e-mail: petr.travnicek@mendelu.cz